

## 미세한 입자의 석회석 slurry 를 이용한

### 아황산 가스의 흡수

표 재 호·정 인 재  
 한국과학기술원 화학공학과

(접수 1981. 4. 8)

## Absorption of Sulfur Dioxide into Slurry Containing Fine Limestone Particles

Jae-Ho Pyo and In-Jae Chung

*Department of Chemical Engineering*

*Korea Advanced Institute of Science and Technology, Seoul, 131, Korea*

(Received April 8, 1981)

### 요 약

미세한 석회석입자를 이용한 아황산가스의 흡수현상을 2 반응면 모델(3영역 모델)을 적용하여 이론적으로 해석하였다. 제안된 모델을 확인하기 위하여, 평평한 기액 계면을 갖는 교반조 흡수기를 사용하여 20°C에서 행한 흡수 실험으로 부터 구해진 액막 물질전달계수에 대한 증진인자(enhan- cement factor) 또는 모델로부터 이론적으로 산출된 값과 비교되었는데, 비교적 좋은 일치를 보였다. 석회석의 용해를 증진시킴으로써 아황산가스 흡수 속도가 증가되었다. 액막의 두께가 석회석 입자보다 훨씬 클 경우,  $\text{CaSO}_3 \cdot \frac{1}{2}\text{H}_2\text{O}$ 의 생성이 석회석입자 표면에 축적되는 현상을 고려해야 함이 제시되었다.

### Abstract

Chemical absorption mechanism of sulfur dioxide into the slurry containing fine limestone particles was analyzed theoretically by a two reaction planes model(three zone model). As an experimental verification of the model, enhancement factors for the liquid film mass transfer coefficients, which were obtained by the absorption using a stirred tank absorber

with a plane gas-liquid interface at 20°C, were compared with the values predicted theoretically. It was shown that the absorption rates can be satisfactorily predicted by the proposed model. The data of absorption rate indicate that it is necessary to enhance the solid dissolution in order to improve the absorption rate. Blinding in the liquid film as well as in the bulk slurry must be considered significantly when the limestone particle is much smaller than the thickness of liquid film.

## I. INTRODUCTION

The removal of sulfur dioxide by absorption using limestone slurry is the most favorable alternative. To design the efficient sulfur dioxide absorber, it may be required to develop a mathematical model which represents the real absorption system. Ramachandran and Sharma<sup>1)</sup> considered, for the first time, the problem of gas absorption accompanied by a fast chemical reaction in a slurry containing sparingly soluble fine particles based on the film concept. Uchida et al.<sup>2),3)</sup> modified the model developed by Ramachandran and Sharma, and they suggested that solid dissolution is enhanced by the reaction between the absorbed gas and the dissolved solid species in the liquid film, and hence, the rate of absorption becomes higher than that predicted by the model of Ramachandran and Sharma. Although the chemical reaction was assumed to be instantaneous in the model of Ramachandran and Sharma and the model of Uchida et al., Sada et al.<sup>4)</sup> extended these models to the process of absorption with a finite rate of reaction into a slurry. They concluded from the experimental results that the extension of the model of Uchida et al. can be satisfactorily applied to the process when compared with the extension of the model of Ramachandran and Sharma.

Recently Sada et al.<sup>5)</sup> proposed the two-reaction-planes model from the fact that the reactions of sulfur dioxide in alkaline slurries are regarded as being consecutive and parallel. The two reaction planes model may be called as a three zone model.<sup>6)</sup>

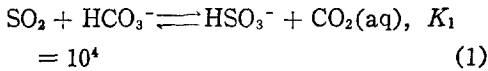
In this study the three zone model is applied to develop a mathematical model for sulfur dioxide absorption into a limestone slurry, and the applicability of the model was examined by the absorption experiment of SO<sub>2</sub> in a stirred tank absorber with a plane gas-liquid interface.

## II. ENHANCEMENT FACTOR DERIVATION

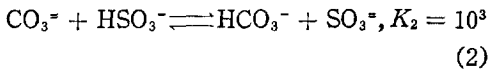
Bjerle et al.<sup>7)</sup> reported their experimental finding that the concentration of HCO<sub>3</sub><sup>-</sup> in limestone slurry in the range of pH 8.3 to 8.5 is in the order of 10<sup>-3</sup> g-mole/l while the concentration of OH is in the order of 10<sup>-6</sup> g-mole/l, which means that HCO<sub>3</sub><sup>-</sup> is the dominant reactant in the reaction with sulfur dioxide. It was found from the literature<sup>8)</sup> that the concentration of HCO<sub>3</sub><sup>-</sup> is about 1.15 × 10<sup>-3</sup> g-mole/l whereas the concentration of CO<sub>3</sub><sup>=</sup> is about 1.65 × 10<sup>-5</sup> g-mole/l when calcium carbonate is saturated in water at 16°C in contact with air including carbon dioxide content of 301 ppm to 327 ppm. Furthermore, the chemical absorption of sulfur dioxide into limestone slurry

gives a considerable amount of carbon dioxide and this helps the concentration of  $\text{HCO}_3^-$  in the bulk slurry remain much higher than that of  $\text{CO}_3^{2-}$ .

The mass transfer in the liquid film is presented qualitatively in *Fig. 1*. The concentration of sulfur dioxide dissolved in the solution is  $C_{Ai}$  at the gas-liquid interface. The aqueous  $\text{SO}_2$  will diffuse toward the liquid and react with the dominant reactant  $\text{HCO}_3^-$  at the first plane  $z_1$  to yield  $\text{HSO}_3^-$  and  $\text{CO}_2$  (aq)



The reaction product  $\text{HSO}_3^-$  will diffuse and react with another reactant  $\text{CO}_3^{2-}$  to yield  $\text{HCO}_3^-$  and  $\text{SO}_3^{2-}$  at the second reaction plane  $z_2$



Most of  $\text{SO}_3^{2-}$  will be converted to  $\text{CaSO}_3 \cdot \frac{1}{2} \text{H}_2\text{O}$  very rapidly by the reaction with  $\text{Ca}^{++}$

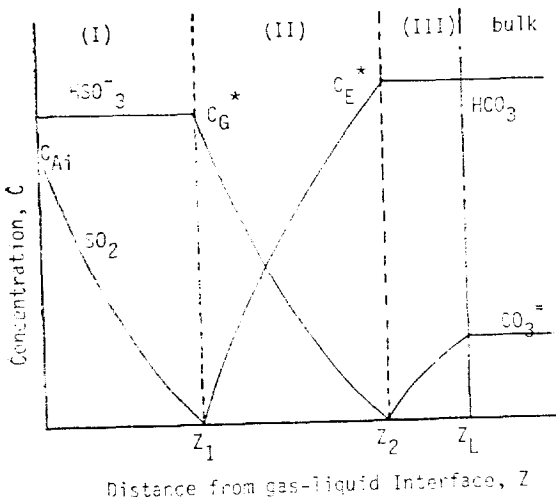
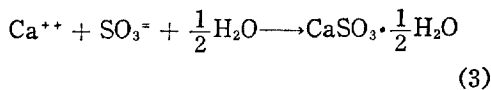


**Fig. 1.** Concentration Profiles for the  $\text{SO}_2\text{-CaCO}_3$  System

All the reactions are considered to be instantaneous and irreversible because the chemical equilibrium constants are very large. It is assumed that the film thickness is much larger than the diameter of limestone particle (usually,  $z_L \geq 10 d_p$ ).<sup>1)</sup> Since the liquid film thickness is much larger than the particle size, the solid dissolution in the liquid film is enhanced by the reaction.

Material balance equations for the relevant species in the zones (I), (II) and (III) depicted in *Fig. 1* are obtained for the steady state.<sup>2)</sup>

In zone (I) the material balance equation for sulfur dioxide is

$$D_A \frac{d^2 C_A}{dz^2} - k_s \left( 1 + \frac{D_A C_A}{D_B C_{B_s}} + \frac{D_G C_G}{D_B C_{B_s}} \right) A_p C_{B_s} = 0 \quad (4)$$

In zone (II) two equations are obtained

$$D_G \frac{d^2 C_G}{dz^2} - k_s \left( 1 + \frac{D_G C_G}{D_B C_{B_s}} \right) A_p C_{B_s} = 0 \quad (5)$$

$$D_E \frac{d^2 C_E}{dz^2} + k_s \left( 1 + \frac{D_G C_G}{D_B C_{B_s}} \right) A_p C_{B_s} = 0 \quad (6)$$

In zone (III) the material balance equation for  $\text{CO}_3^{2-}$  is

$$D_B \frac{d^2 C_B}{dz^2} + k_s (C_{B_s} - C_B) A_p = 0 \quad (7)$$

The second terms in equations (4), (5) and (6) represent the rate of consumption or production of components  $\text{SO}_2$ ,  $\text{HSO}_3^-$  and  $\text{HCO}_3^-$  by the limestone dissolution in the liquid film. The second term in equation (7) denotes the rate of solids dissolution.

Equations from (4) to (7) can be solved by the aid of the following boundary conditions

$$z = 0 : C_A = C_{Ai}, C_G = C_{G^*} \quad (8)$$

$$z = z_1 : C_A = C_E = 0, C_G = C_{G^*} \quad (9)$$

$$-D_A \frac{dC_A}{dz} = D_E \frac{dC_E}{dz} = -D_G \frac{dC_G}{dz} \quad (10)$$

$$z = z_2 : C_B = C_G = 0, C_E = C_{E^*} = C_{E0} \quad (11)$$

$$D_B \frac{dC_B}{dz} = -D_G \frac{dC_G}{dz} = D_E \frac{dC_E}{dz} \quad (12)$$

and

$$z = z_L : C_B = C_{B0}, C_E = C_{E0} \quad (13)$$

All the above equations and boundary conditions are put into the dimensionless form.

In zone (I)

$$\frac{d^2 Y_A}{dx^2} - N \left( \frac{1}{r_{AQA}} + \frac{r_G}{r_{AQA}} Y_G + Y_A \right) = 0 \quad (14)$$

In zone (II)

$$\frac{d^2 Y_G}{dx^2} - N \left( \frac{1}{r_G} + Y_G \right) = 0 \quad (15)$$

and

$$\frac{d^2 Y_E}{dx^2} + N \left( \frac{1}{r_E} + \frac{r_G}{r_E} Y_G \right) = 0 \quad (16)$$

In zone (III)

$$\frac{d^2 Y_B}{dx^2} + N(1 - Y_B) = 0 \quad (17)$$

$$\phi_A = \frac{\dot{k}_{l,A}}{k_{l0,A}} = - \left. \frac{dY_A}{dx} \right|_{x=0} = \frac{\{1 + (1 + r_G Y_G^*) / (r_{AQA})\} \sqrt{N} \cosh(\sqrt{N} x_1) - (1 + r_G Y_G^*) \sqrt{N} / (r_{AQA})}{\sinh(\sqrt{N} x_1)} \quad (24)$$

Unknown values of  $x_1$  and  $Y_G^*$  can be calculated from the following equations, which

$$\begin{aligned} & \frac{(r_{AQA} + 1 + r_G Y_G^*) \sqrt{N} - (1 + r_G Y_G^*) \sqrt{N} \sinh(\sqrt{N} x_1)}{\sinh(\sqrt{N} x_1)} \\ &= \frac{-\sqrt{N} [1 - (1 + r_G Y_G^*) \cosh\{\sqrt{N}(x_2 - x_1)\}]}{\sinh\{\sqrt{N}(x_2 - x_1)\}} + \frac{r_E Y_{E0} - r_G Y_G^*}{x_2 - x_1} \\ &= \frac{-\sqrt{N} [1 - (1 + r_G Y_G^*) \cosh\{\sqrt{N}(x_2 - x_1)\}]}{\sinh\{\sqrt{N}(x_2 - x_1)\}} \end{aligned} \quad (25)$$

and

$$\begin{aligned} & \frac{\sqrt{N} \cosh\{\sqrt{N}(1 - x_2)\} - (1 - Y_{B0}) \sqrt{N}}{\sinh\{\sqrt{N}(1 - x_2)\}} = \frac{-\sqrt{N} [\cosh\{\sqrt{N}(x_2 - x_1)\} - 1 - r_G Y_G^*]}{\sinh\{\sqrt{N}(x_2 - x_1)\}} \\ &= \frac{-\sqrt{N} [\cosh\{\sqrt{N}(x_2 - x_1)\} - 1 - r_G Y_G^*]}{\sinh\{\sqrt{N}(x_2 - x_1)\}} + \frac{r_E Y_{E0} - r_G Y_G^*}{x_2 - x_1} \end{aligned} \quad (26)$$

### III. EXPERIMENTAL

The schematic diagram of absorption system is shown in Fig. 2. Nitrogen gas from nitrogen cylinder is passed through the water vapor saturator and mixed with sulfur dioxide gas from SO<sub>2</sub> cylinder thoroughly at

The dimensionless boundary conditions are

$$x = 0 : Y_A = 1, Y_G = Y_G^* \quad (18)$$

$$x = x_1 : Y_A = Y_E = 0, Y_G = Y_G^* \quad (19)$$

$$-r_{AQA} \frac{dY_A}{dx} = r_E \frac{dY_E}{dx} = -r_G \frac{dY_G}{dx} \quad (20)$$

$$x = x_2 : Y_B = Y_G = 0, Y_E = Y_E^* = Y_{E0} \quad (21)$$

$$\frac{dY_B}{dx} = -r_G \frac{dY_G}{dx} = r_E \frac{dY_E}{dx} \quad (22)$$

$$x = 1 : Y_B = Y_{B0}, Y_E = Y_{E0} \quad (23)$$

The enhancement factor for the liquid film mass transfer coefficient can be determined theoretically from equations (14)-(17) with the boundary conditions (18)-(23)

are given by the boundary conditions (20) and (22)

the mixing column. The gas mixture enters the stirred tank absorber, where sulfur dioxide is removed from the gas mixture into limestone slurry. The exit gas of the absorber is discharged to the vent. Limestone slurry is fed to the absorber from the slurry feed tank. The whole system was maintained at 20(±1)°C.

The stirred tank absorber with a plane gas-liquid interface was used for all the experiments. The vessel was made of acrylic resin except for top and bottom plates and has four equally spaced baffles attached to the internal wall of the liquid phase. The liquid phase volume was 2180 cm<sup>3</sup> and the gas phase volume was 1260 cm<sup>3</sup>. Two stirrers were used for agitation in the gas and liquid, driven by two separate motors. Agitator impeller speed in gas phase was fixed at 320 rpm, and the liquid side stirrer was driven at two constant speeds of 50 rpm and 67 rpm.

Prior to the chemical absorption experiments, the physical absorption of pure CO<sub>2</sub> into water was done to determine the mass transfer coefficient in liquid film using the stirred tank absorber. To measure the concentration of CO<sub>2</sub> in water, an excess amount

of 20 mM-Ba(OH)<sub>2</sub> solution was added to the sample and it was back titrated with 20 mM-HCl solution by using phenolphthalein solution as an indicator.<sup>10)</sup>

Mass transfer coefficient in gas phase was obtained by absorbing lean SO<sub>2</sub> gas diluted with nitrogen into 1 M-NaOH solution in the stirred tank absorber. The compositions and flow rates of the inlet and outlet gas mixtures of the absorber were measured.

The experiments for the absorption of SO<sub>2</sub> into the limestone slurry were performed under various conditions. The range of SO<sub>2</sub> concentration in the inlet gas mixture was from 4,000 to 20,000 ppm and slurry concentrations were fixed at 1, 2 and 5 weight percent. The flow rate of gas mixture was always about 1,062 cm<sup>3</sup>/min and the loading volume of slurry was 2,180 cm<sup>3</sup>. The gas

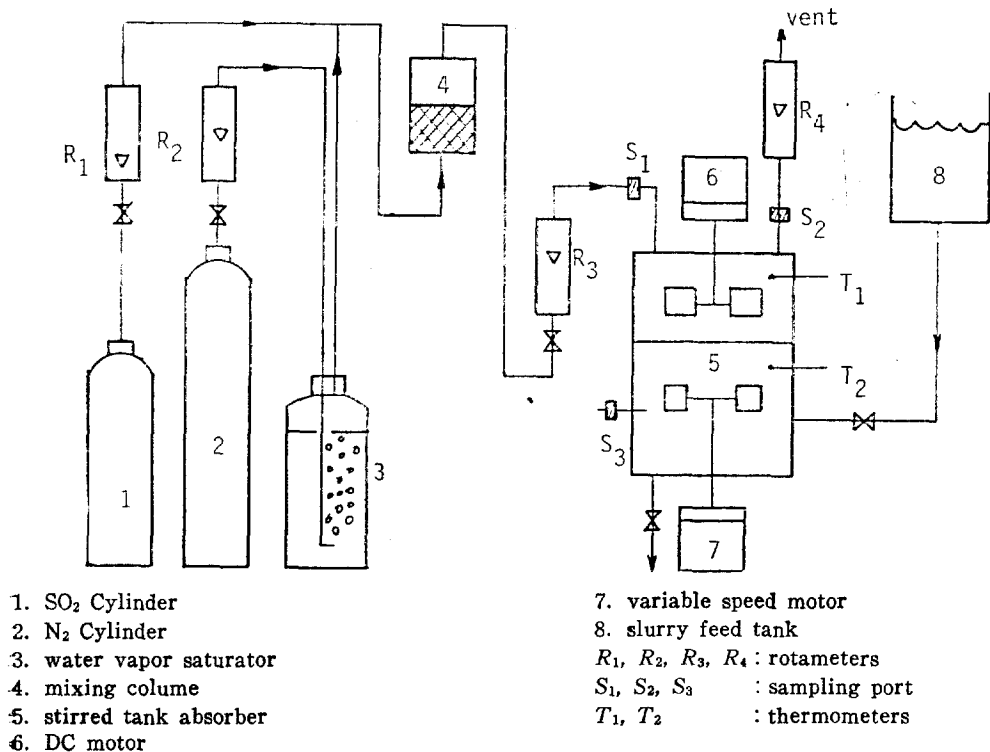


Fig. 2. Schematic Diagram of Experimental Apparatus

samples were taken when the pH value of the slurry was placed in the range of 8.0 to 8.4. and then the slurry was replaced by the fresh for the next experiment run.

To investigate the effect of pH on the absorption, the SO<sub>2</sub> concentration of inlet gas was fixed at 6,800 ppm and the speed of liquid side stirrer at 67 rpm. The experiment was carried out by the batch operation.

Gas side concentrations of SO<sub>2</sub> and CO<sub>2</sub> were measured using the Varian 920 gas chromatograph. The column was packed with porapak Q.

### IV. RESULTS AND DISCUSSION

#### (1) Mass Transfer Coefficients for Physical Absorption

The gas film mass transfer coefficient of sulfur dioxide was calculated from the material balance equation for sulfur dioxide in the experiment of lean SO<sub>2</sub> gas absorption into 1 M-NaOH solution.

$$R_A = Q(P_{Af} - P_{Ag}) / (RTA) = k_g P_{Ag} \quad (27)$$

The liquid film mass transfer coefficient of CO<sub>2</sub> was calculated from the following equation

$$\ln \left\{ \frac{(C_{Ff} - C_{F1})}{(C_{Ff} - C_{F2})} \right\} = k_{l0,F} A (t_2 - t_1) / V \quad (28)$$

And then the coefficient of SO<sub>2</sub> was obtained from the following correlation<sup>11)</sup>

$$k_{l0,A} = k_{l0,F} (D_A / D_F)^{2/3} \quad (29)$$

The surface area of the solid particles per unit volume of the slurry was approximately obtained from the following relation

$$A_p = 6W / (\rho_p d_p) \quad (30)$$

The mass transfer coefficient for the limestone dissolution  $k_s$  was estimated by the Hixson's correlation<sup>12)</sup>

$$k_s D_t / D_B = 0.16 (Re_t)^{0.62} (\mu_L / \rho_L D_B)^{0.5}$$

$$\text{for } Re_t > 6.7 \times 10^4 \quad (31)$$

$$k_s D_t / D_B = 2.7 \times 10^{-5} (Re_t)^{1.4} (\mu_L / \rho_L D_B)^{0.5}$$

$$\text{foe } Re_t < 6.7 \times 10^4 \quad (32)$$

where  $k_s$  was assumed to be independent of the particle size and physical properties of  $\mu_L$  and  $\rho_L$  were considered to be the same as those of water.

#### (2) Absorption of Sulfur Dioxide into Limestone Slurry

The experimental enhancement factor,  $\phi_{A,exp}$ , was calculated from the following equation

$$R_A = Q(P_{Af} - P_{Ag}) / (RTA) = k_g (P_{Ag} - P_{Ai}) = \phi_{A,exp} k_{l0,A} C_{Ai} \quad (33)$$

where  $C_{Ai}$  was calculated from the equilibrium relation for pure water absorbent propose by Fujita<sup>13)</sup>

$$C_{Ai} = (23.067 P_{Ai} + d.2835 P_{Ai}) / 18 \quad (34)$$

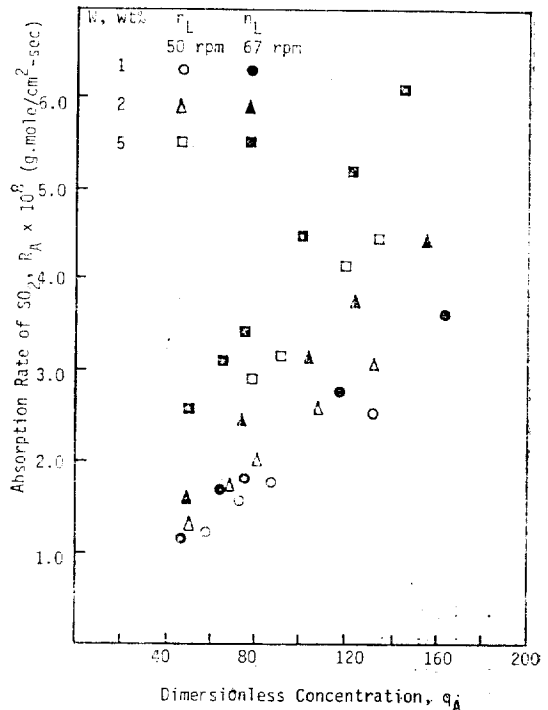


Fig. 3. Absorption Rate of SO<sub>2</sub> at Various Conditions

Diffusivities in the limestone slurry were assumed to be the same as those in water.

Fig. 3 shows that the absorption rate of sulfur dioxide increases remarkably as the solid concentration and the speed of liquid side stirrer increase, which means that solid dissolution plays a very important role in the absorption. In order to improve the absorption rate, it may be necessary to enhance the solid dissolution.

Enhancement factors for the liquid film mass transfer coefficients are plotted as a function of two dimensionless parameters,  $N$  and  $q_A$ , in Fig. 4. The experimental enhancement factors show fairly good agreement with theoretical ones predicted by the proposed model. This implies that the absorption rate of  $SO_2$  into limestone slurry can be satisfactorily evaluated by the proposed three zone model. It is shown that the predicted enhancement factor is generally a bit higher than the observed one. It is believed that the crystallization of  $CaSO_3 \cdot \frac{1}{2}H_2O$  on the surface of limestone particle may cause the inhibition from further solid dissolution. This phenomenon is called a blinding. The deviation of theoretical factor from experimental one is larger for higher concentration of limestone and/or lower speed of stirrer. It is considered that such a result is probably owing to the difficulty of complete mixing of the limestone particles in the slurry, especially near the gas-liquid interface.

Absorption rates of sulfur dioxide are plotted against various values of pH in Fig. 5. The absorption rate is slightly dependent on the pH in the pH range of 7.0 to 8.2, and it decreases rather steeply below the pH values of 7. Considering that the experiment was carried out in batch operation with re-

spect to the slurry, accumulation of blinded limestone particles in the slurry may be a major cause of such a result.

Below the pH value of 6.0, a large portion of  $SO_3^{2-}$  ion produced from the dissolution of  $CaSO_3 \cdot \frac{1}{2}H_2O$  will convert rapidly to  $HSO_3^-$  ion, leading to decrease the absorption rate.<sup>14)</sup> Therefore, the reaction mechanism at the

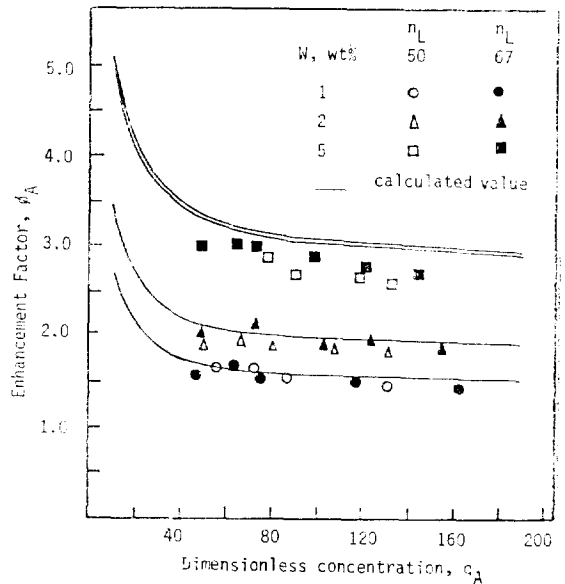


Fig. 4. Enhancement Factor for Different Dimensionless Concentration

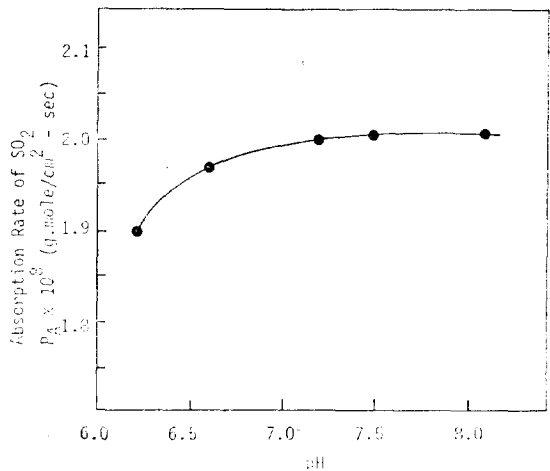


Fig. 5. pH Effect on Absorption Rate of  $SO_2$  (Inlet  $SO_2$  Conc. 6800 ppm, 2 wt%  $CaCO_3$  slurry,  $n_L = 67$  rpm)

reaction plane should be modified at the low pH.

## CONCLUSION

The absorption rate of  $\text{SO}_2$  into a limestone slurry was analyzed theoretically using a three zone model. The agreement between theoretical and experimental enhancement factors was fairly good. When the limestone concentration is high, a slight discrepancy between them is shown. This may suggest that an experimental device for complete mixing of limestone particles is required. The data of absorption rate indicate that it may be necessary to enhance the solid dissolution in order to improve the absorption rate. Blinding in the liquid film as well as in the bulk slurry must be considered significantly when the size of limestone particle is much smaller than the thickness of liquid film.

## NOMENCLATURE

$A$ : gas-liquid interfacial area ( $\text{cm}^2$ )  
 $A_p$ : surface area of solid particles per unit volume of slurry ( $\text{cm}^2/\text{cm}^3\text{-slurry}$ )  
 $C_{Fi}$ : concentration of species  $F$  at time  $t_i$  ( $\text{g-mole}/\text{cm}^3$ )  
 $C_j$ : concentration of species  $j$  in liquid phase ( $\text{g-mole}/\text{cm}^3$ )  
 $D_j$ : diffusivity of species  $j$  in liquid phase ( $\text{cm}^2/\text{sec}$ )  
 $D_t$ : diameter of stirred tank absorber (cm)  
 $d_p$ : average diameter of the limestone particles (cm)  
 $K_i$ : chemical equilibrium constant for reaction (i)  
 $k_s$ : mass transfer coefficient of species  $A$  in gas phase ( $\text{g-mole}/\text{cm}^2\text{-sec-atm}$ )

$k_l$ : mass transfer coefficient for liquid phase ( $\text{cm}/\text{sec}$ )  
 $k_{l0}$ : mass transfer coefficient in liquid phase for physical absorption ( $\text{cm}/\text{sec}$ )  
 $k_s$ : mass transfer coefficient for limestone dissolution ( $\text{cm}/\text{sec}$ )  
 $n_L$ : speed of liquid-side stirrer (rpm)  
 $N$ :  $k_s A_p z_L / D_B$   
 $P_j$ : partial pressure of species  $j$  in gas phase (atm)  
 $Q$ : gas flow rate ( $\text{cm}^3/\text{sec}$ )  
 $q_A$ : dimensionless concentration,  $C_{Ai}/C_{Bi}$   
 $R$ : gas constant ( $82.05 \text{ cm}^3\text{-atm}/\text{g-mole } ^\circ\text{K}$ )  
 $R_A$ : absorption rate of species  $A$  ( $\text{g-mole}/\text{cm}^2\text{-sec}$ )  
 $Re_t$ : Reynolds number for liquid phase,  $D_t^2 n_L \rho_L / \mu_L$   
 $r_j$ : dimensionless diffusivity of species  $j$ ,  $D_j / D_B$   
 $T$ : absolute temperature ( $^\circ\text{K}$ )  
 $t_i$ : time (sec)  
 $V$ : volume of liquid in stirred tank absorber ( $\text{cm}^3$ )  
 $W$ : limestone concentration ( $\text{g}/\text{cm}^3\text{-slurry}$  or wt%)  
 $x$ : dimensionless distance from gas-liquid interface  
 $x_1, x_2$ :  $z_1/z_L$  and  $z_2/z_L$  respectively  
 $Y_A$ : dimensionless concentration of species  $A$ ,  $C_A/C_{Ai}$   
 $Y_j$ : dimensionless concentration of species  $j$ ,  $C_j/C_{Bi}$   
 $z$ : distance from gas-liquid interface into liquid phase (cm)  
 $z_1, z_2$ : position of reaction plane in the liquid film (cm)  
 $z_L$ : thickness of liquid film for gas absorption (cm)

## Greek Symbols

$\mu_L$ : viscosity of liquid ( $\text{g}/\text{cm-sec}$ )

$\rho_L, \rho_p$  : densities of liquid and limestone particle (g/cm<sup>3</sup>)

$\phi_A$  : enhancement factor of species A absorption

### Subscripts and Superscripts

A : SO<sub>2</sub>

B : CO<sub>3</sub><sup>-</sup>

E : HCO<sub>3</sub><sup>-</sup>

F : CO<sub>2</sub>

G : HSO<sub>3</sub><sup>-</sup>

f : feed to stirred tank absorber

g : gas phase value

i : at gas-liquid interface

s : at the surface of limestone particle

o : in bulk of slurry

\* : at reaction plane

### References

1. P.A. Ramachandran and M.M. Sharma, Chem. Eng. Sci., (1969), 1681.
2. S. Uchida, et al., Chem. Eng. Sci., 30 (1975), 644.
3. S. Uchida, et al., Chem. Eng. Sci., 32 (1977), 447.
4. E. Sada, et al., Chem. Eng. Sci., 32(1977), 1165.
5. E. Sada, et al., Chem. Eng. Journal, 19 (1980), 131.
6. G.R. Charmichael and S.C. Chang, Chem. Eng. Sci., 35(1980), 2463.
7. I. Bjerle, et al., Chem. Eng. Sci., 27 (1972), 1853.
8. W.F. Linke and A. Seidell, "Solubilities of Inorganic and Metal Organic Compounds," Vol. 1, American Chemical Society, Washington, D.C., 1958.
9. J.H. Pyo, M.S. Thesis, KAIST, Korea (1981).
10. S. Uchida, et al., Can. J. Chem. Eng., 56 (1978), 690.
11. H. Hikita, et al., Chem. Eng. Sci., 30 (1975), 607.
12. S. Boon-Long, et al., Chem. Eng. Sci., 33(1978), 813.
13. S. Fujida, Kagaku Kogaku, 27(1963), 112.
14. J.M. Potts, et al., 2nd Int. Lime/Limestone Wet Scrubbing Sym. (1971).

